Nanoscience and Nanotechnology: An Indian Journal

Research Article | Vol 17 Iss 1

Relative Humidity Monitoring of Ag-Doped TiO_2

Anupam Kumar Tripathi[1*], **Anoop Kumar**[2]

[1] Department of Physics, Faculty of Engineering & Technology, University of Lucknow, Lucknow, U.P., India

[2] Department of Physics, University of Lucknow, Lucknow, U.P., India

[*]**Corresponding author**: Anupam Kumar Tripathi, Department of Physics, Faculty of Engineering & Technology, University of Lucknow, Lucknow U.P. India **E-mail:** tripathi198117@gmail.com.

Received date: 16-March-2023, Manuscript No. tsnsnt-23-92675; **Editor assigned:** 18-March-2023, PreQC No. tsnsnt-23-92675 (PQ); **Reviewed:** 21-March-2023, QC No. tsnsnt-23-92675 (Q); **Revised:** 24-March-2023, Manuscript No. tsnsnt-23-92675 (R); **Published:** 31-March-2023. DOI: 10.37532/0974-7494.2023.17(1).187

ABSTRACT

Practical applications of TiO_2 are limited due to its wide band gap and fast recombination of electron-hole pairs within nanoseconds. So far numerous researches have been focused on defeating these disadvantages by introducing noble metals into titania lattice. Noble metals deposited or doped in TiO_2 have high Schottky barriers among the metals and act as electron traps, facilitating electron-hole separation and promoting the interfacial electron transfer process. These additives capture electrons resulting in a lower recombination rate of electron-hole pairs. However, some noble metals such as Pt, Pd, Rh, and Au are too expensive to be used on the industrial scale. Therefore, the research on Ag-doped TiO_2 has significant practical value. Silver is suitable for industrial applications due to its comparable cost and easy preparation. It is a suitable element, which improves the TiO_2 photo-catalytic performance, it is also believed that the silver ions interact with sulfur, oxygen, and nitrogen in the molecules of microorganisms and inactivate the cellular proteins resulting in titania as better bioactive material. Ag-doped titania layers with different morphologies have been grown by the Sol-gel method.

Keywords: ***Bioactive material, Electron-hole recombination, Humidity sensors, Photo-catalytic performance***

Introduction

Practical applications of TiO_2 are limited due to its wide band gap and fast recombination of electron-hole pairs within nanoseconds. So far numerous researches have been focused on defeating these disadvantages by introducing noble metals into titania lattice. Noble metals deposited or doped in TiO_2 have high Schottky barriers among the metals and act as electron traps, facilitating electron-hole separation and promoting the interfacial electron transfer process. These additives capture electrons resulting in a lower recombination rate of electron-hole pairs (227). However, some noble metals such as Pt, Pd, and Au are too expensive to be used on the industrial scale.

Therefore, the research on Ag-doped TiO_2 has significant practical value. Silver is suitable for industrial applications due to its comparable cost and easy preparation. It is a suitable element that improves the TiO_2 photo-catalytic performance, it is also believed that the silver ions interact with sulfur, oxygen, and nitrogen in the molecules of microorganisms and inactivate the cellular proteins resulting in titania as better bioactive material. Ag-doped titania layers with different morphologies have been grown by the Sol-gel method.

As the Fermi levels of these noble metals are lower than that of TiO_2, photoexcited electrons can be transferred from the conduction band to the metal particles deposited on the surface of TiO_2, while photogenerated valence holes remain in

Citation: Tripathi A.K., Kumar A. Relative Humidity Monitoring of Ag Doped TiO_2. Nano Tech Nano Sci IndJ.2023;17(1):187

TiO_2. These activities greatly reduce the possibility of electron-hole recombination, resulting in efficient separation and stronger photo-catalytic reactions [1].

Experimental Procedure

The synthesized TiO_2 powder was doped with Ag with 20 wt% and made fine by grinding it in a mortar with a pestle for 2 hrs. The pellet of this material having dimensions 9 mm in diameter and 3 mm in thickness, has been made by hydraulic pressing machine (M.B. Instruments, Delhi, India) under the pressure of 616 M Pa at room temperature. This pellet TA-20 was annealed in an electric muffle furnace (Ambassador, India) at 500°C, 600°C, and 700°C for 3 hrs successively and after each annealing process exposed to humidity in the humidity chamber. Inside the humidity chamber, a thermometer (± 10°C) and standard hygrometer (Huger, Germany, ± 1RH%) are placed for the purpose of calibration. Variation in resistance was recorded with the change in relative humidity. The pellet's resistance variation was recorded using a resistance meter (Sino meter ±0.001MΩ, Model: VC 9808). The copper electrode was used to measure the resistance of the pellet.

The specific Sensitivity of the sensor is defined as the change in resistance (ΔR) of the sensing element per unit change in relative humidity (RH %) per unit resistance, i.e.

$$\Delta S = \Delta R / R\ (\Delta\ RH\ \%) \qquad (1)$$

After studying humidity-sensing properties, sensing elements were kept in the laboratory environment, and their humidity-sensing characteristics were regularly monitored. The effect of aging on the sensing properties of these elements was examined again in the humidity chamber after six months of fabrication of the pellet for the stability analysis of the sensor [2].

Study of Surface morphology

XRD Study of Ag-doped TiO_2: The XRD pattern of Ag-doped TiO_2 annealed at 500ºC, 600ºC, and 700ºC is shown in **FIG. 1-3.** X-ray Diffraction by X-Pert PRO XRD system (Netherland) shows the extent of crystallization of the sensing element as shown in **TABLE 1.**

The average crystallite size has been calculated using the Debye-Scherer formula. The minimum crystallite size is 108 nm at 600ºC [3,4].

TABLE 1. **XRD Study of Ag doped TiO_2.**

Ag doped TiO_2 annealed at 500ºC		**Ag doped TiO_2 annealed at 600ºC**		**Ag doped TiO_2 annealed at 700ºC**	
Average crystallite size is 116 nm		**Average crystallite size is 108 nm**		**Average crystallite size is 119 nm**	
2θ values	**Corresponding Miller Planes**	**2θ values**	**Corresponding Miller Planes**	**2θ values**	**Corresponding Miller Planes**

25.28º 36.88º 38.09º 44.23º 47.85º 49.88º 54.86º 62.66º	(101) (103) (111) (200) (002) (020) (105) (204)	25.38º 37.04º 38.19º 44.41º 48.05º 53.99º 55.14º 62.78º	(101) (-205) (111) (200) (021) (105) (211) (002)	25.71º 28.71º 34.10º 35.71º 41.74º 49.98º 54.64º 55.79º	(101) (200) (002) (-202) (-331) (122) (131) (421)

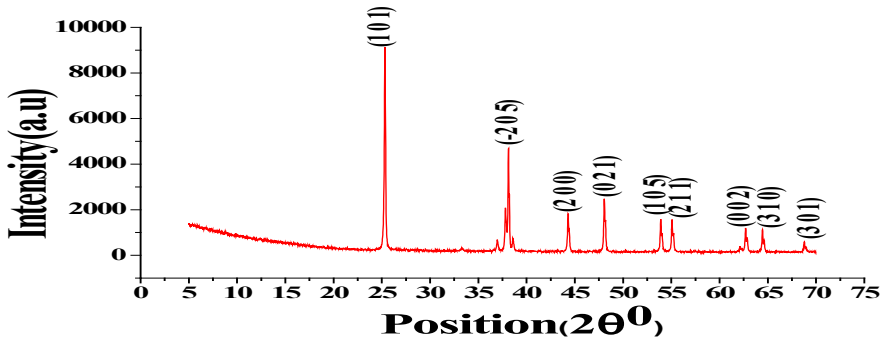

FIG. 1. **XRD pattern of sensing element TA-20 annealed at 500°C.**

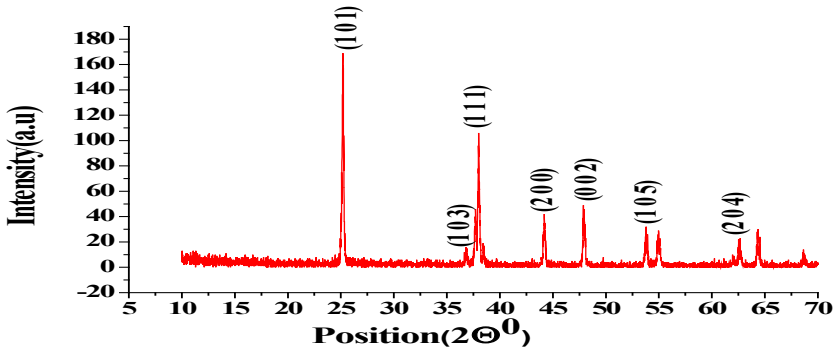

FIG. 2. **XRD pattern of sensing element TA-20 annealed at 600 ⁰C.**

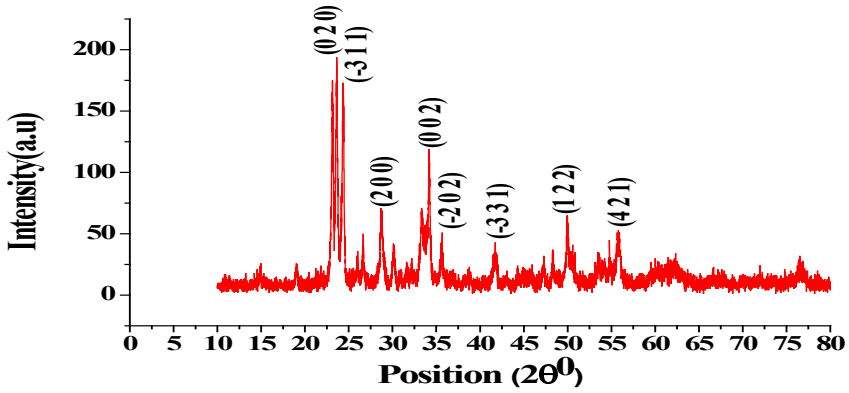

FIG. 3. **XRD pattern of sensing element TA-20 annealed at 700ºC.**

Scanning electron microscopy

Surface morphology was studied using Scanning Electron Microscope Unit (SEM, LEO-0430, Cambridge). SEM micrograph shows that grains are of nano-size and the surface is porous in nature. These pores are expected to provide sites for humidity adsorption. The structure favors the adsorption and condensation of water vapors. The surface morphology of sensing elements TA-20 annealed at 700°C was studied. The grain size of sensing element TA-20 annealed at 700°C is found to be 98 nm. It shows uniform distribution of particles having an approximately rounded shape [5,6].

Fourier Transform Infrared Spectroscopy (FTIR)

FTIR spectra were recorded by KBr disc on Tensor-27 Spectrum. IR spectroscopy was used for understanding the nature of organics present in the final products. FTIR absorption peaks shown in **FIG. 4** for the samples show positive agreement when compared with data in infrared spectra of inorganic compounds [7,8]. The peaks of pure TiO_2 were observed at 609 cm^{-1}, 1130 cm^{-1}, and 1409 cm^{-1} whereas the peaks of TiO_2-Ag were 1335 cm^{-1} and 2360 cm^{-1}.

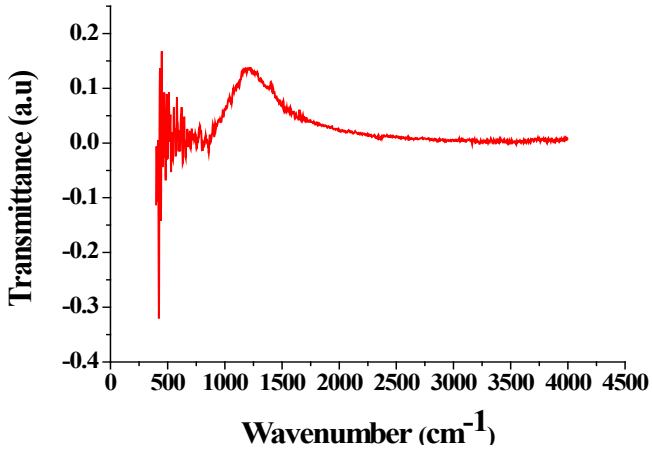

FIG 4. **FTIR spectrum of the sensing element TA-20 annealed at 700⁰C**

Result and Discussion

Resistance of the sample pellet T-20 has been measured after each time of annealing during controlled exposure to humidity in the

range of 5% to 95%. Variation of resistance with a change in relative humidity at temperatures 500°C, 600°C, and 700°C of sample T-20 in **FIG. 5-8** [9-12].

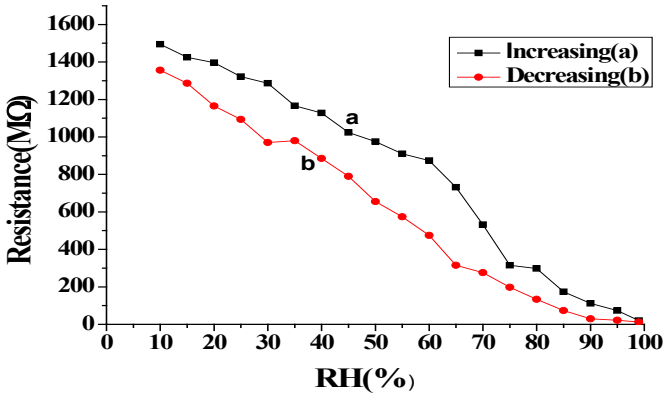

FIG. 5**. Hysteresis graph for the sensing element TA-20 annealed at 500˚C.**

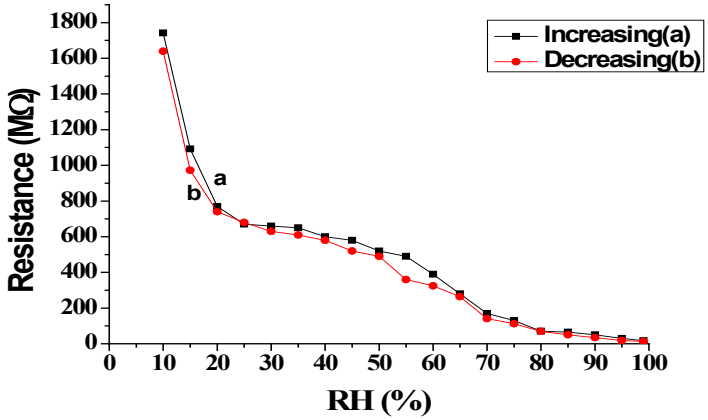

FIG. 6. **Hysteresis graph for the sensing element TA-20 annealed at 600˚C.**

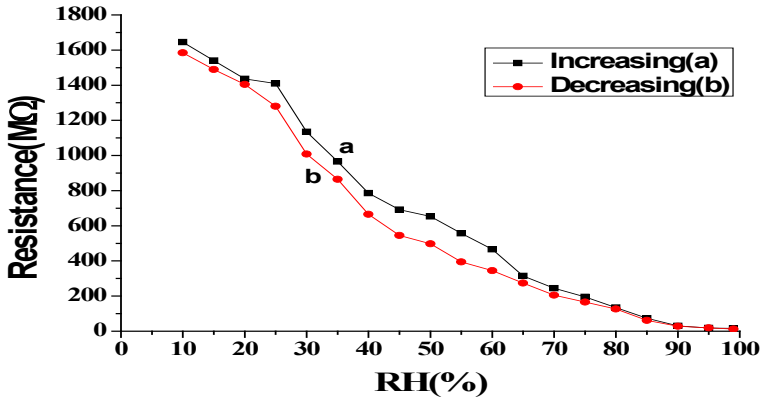

FIG. 7. **Hysteresis graph for the sensing element TA-20 annealed at 700˚C.**

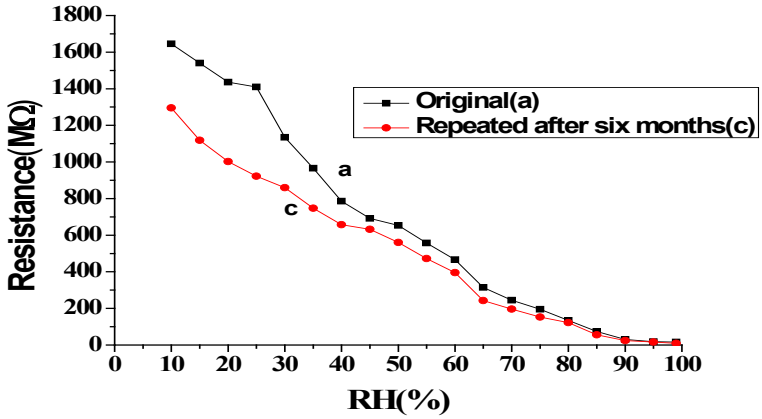

FIG. 8. **Repeatability graph for six months at sensing element TA-20 annealed at 700°C.**

Conclusion

As the Fermi levels of these noble metals are lower than that of TiO_2, photo-excited electrons can be transferred from the conduction band to the metal particles deposited on the surface of TiO_2, while photo-generated valence holes remain in the TiO_2. These activities greatly reduce the possibility of electron-hole recombination, resulting in efficient separation and stronger photo-catalytic reactions.

REFERENCES

1. Kulwicki BM. Humidity sensors. J Am Ceram Soc. 1991; 74(4):697-708.
2. Mistry KK, Saha D, Sengupta K. Sol–gel processed Al2O3 thick film template as sensitive capacitive trace moisture sensor. Sens Actuators B: Chem. 2005; 106(1): 258-62.
3. Kummer AM, Hierlemann A. Configurable electrodes for capacitive-type sensors and chemical sensors. IEEE Sens J. 2006; 6(1):3-10.
4. Bayhan M, Hashemi T, Brinkman AW. Sintering and humidity-sensitive behaviour of the ZnCr2O4–K22CrO4 ceramic system. Journal of Materials Science. 1997; 32:6619-23.
5. Traversa E. Ceramic sensors for humidity detection: the state-of-the-art and future developments. Sens Actuators B Chem. 1995;23(2-3):135-56.
6. Yeh YC, Tseng TY, Chang DA. Electrical properties of TiO_2-K2Ti6O13 porous ceramic humidity sensor. J Am Ceram. Soc. 1990;73(7):1992-8.
7. Wu L, Wu CC, Wu MM. Humidity sensitivity of Sr (Sn, Ti) O_3 ceramics. Journal of electronic materials. 1990;19:197-200.
8. Nitta T, Terada Z, Hayakawa S. Humidity-Sensitive Electrical Conduction of MgCr2O4-TiO2 Porous Ceramics. J Am Ceram. Soc. 1980; 63(5-6):295-300.
9. Chachulski B, Gebicki J, Jasinski G, et al. Properties of a polyethyleneimine-based sensor for measuring medium and high relative humidity. Meas Sci Technol. 2005; 17(1):12.
10. Yadav BC, Pandey NK, Srivastava AK, et al. Optical humidity sensors based on titania films fabricated by sol–gel and thermal evaporation methods. Meas Sci Technol. 2006; 18(1):260.
11. Pandey NK, Tripathi A, Tiwari K, et al. Morphological and humidity sensing studies of WO3 mixed with ZnO and TiO2 powders. Sensors and Transducers. 2008; 96(9):42-6.
12. Parvatikar N, Jain S, Khasim S, et al. Electrical and humidity sensing properties of polyaniline/WO3 composites. Sens Actuators B Chem. 2006; 114(2):599-603.